

Demonstration of Si-doped Al-rich thin regrown Al(Ga)N films on AlN on sapphire templates with $>10^{15}/\text{cm}^3$ free carrier concentration using close-coupled showerhead MOCVD reactor

Swarnav Mukhopadhyay, Parthasarathy Seshadri, Mobinul Haque, Shuwen Xie, Ruixin Bai, Surjava Sanyal, Guangying Wang, Chirag Gupta, Shubhra S. Pasayat

Department of Electrical and Computer Engineering, University of Wisconsin-Madison, Madison, WI, 53706, USA

Abstract:

Thin Si-doped Al-rich ($\text{Al}>0.85$) regrown Al(Ga)N layers were deposited on AlN on Sapphire template using metal-organic chemical vapor deposition (MOCVD) techniques. The optimization of the deposition conditions such as temperature, V/III ratio, deposition rate, and Si concentration resulted in a high charge carrier concentration ($> 10^{15} \text{ cm}^{-3}$) in the Si-doped Al-rich Al(Ga)N films. A pulsed deposition condition was employed to achieve a controllable Al composition greater than 95% and to prevent unintended Ga incorporation in the AlGa_xN material deposited using the close-coupled showerhead reactor. Also, the effect of unintentional Si incorporation on free charge carrier concentration at the regrowth interface was studied by varying the thickness of the regrown Al(Ga)N layer. A maximum charge carrier concentration of $4.8 \times 10^{16} / \text{cm}^3$ and $7.5 \times 10^{15} / \text{cm}^3$ were achieved for Al_{0.97}Ga_{0.03}N and AlN films with thickness < 300 nm compared to previously reported n-Al(Ga)N films with thickness ≥ 400 nm deposited using MOCVD technique.

High-performance power devices with voltage handling capabilities of several kVs are currently in high demand in the power electronics industry. The ultrawide bandgap (UWBG) semiconductors such as Al-rich Al(Ga)N have shown numerous promise for high-voltage operation¹⁻⁶. Similarly, Al(Ga)N-based deep ultra-violet (DUV) emitters, such as light emitting diodes (LEDs) and laser diodes (LDs) are also showing promising performance⁷⁻¹⁰. However, the performance enhancement of both the power and optoelectronic devices requires adequate control of doping into the Al-rich AlGa_xN films. The Al-rich AlGa_xN films with Al content $> 85\%$ suffer from the low conductivity of the film due to higher activation energy of n and p-type dopants, such as Si and Mg, respectively¹¹⁻¹⁵. Furthermore, the Si-doped Al-rich Al_xGa_{1-x}N ($x > 0.85$) films tend to show self-compensation and DX center formation of the dopants which limits the availability of the free charge carrier in the film¹⁶⁻¹⁸. It is also reported that the cation vacancy (V_{III}) complex formation with Si ($V_{\text{III}}\text{-Si}$), which behaves like an acceptor trap state is also a conductivity limiting factor^{11,16}. Apart from that, the Al(Ga)N deposited using the metal-organic chemical vapor deposition (MOCVD) technique suffers from the presence of carbon (C), which is known to act as a compensating acceptor (C_{N})¹¹. It was demonstrated that the optimized deposition condition for reducing the formation energy of the $V_{\text{III}}\text{-Si}$ complex requires a lower deposition temperature, whereas the reduction of the C_{N} formation in the Al(Ga)N needs a high deposition temperature¹⁹. So, a trade-off must be created to obtain highly conductive films. Si-

doped AlN films (Al-polar and N-polar) deposited using molecular beam epitaxy (MBE) exhibit high free carrier concentration ($>10^{18}/\text{cm}^3$) due to their metal-rich growth condition and low deposition temperature compared to MOCVD, reducing the V_{III}-Si formation and enhancing the free-carrier concentration^{12,20}. However, using a similar deposition method with MOCVD is challenging.

Although a significant amount of research has been done on the deposition technique of Si-doped Al-rich (>85%) Al(Ga)N material using vertical and horizontal MOCVD reactors, very few reports have been published for the deposition technique of Al-rich Al(Ga)N materials using close-coupled showerhead (CCS) reactors^{21,22}. The CCS reactors are widely accepted for commercially producing III-nitride films and are easily scalable²³. However, the CCS reactors are known to have issues with unintentional Ga incorporation^{23,24}, which makes it difficult to obtain a controllable Al composition >95% in AlGaN. Since AlN has low n-type conductivity, depositing 95-97% AlGaN may offer better n-type conductivity while minimizing lattice mismatch with AlN buffer layers or the substrate. Also, AlGaN thin films with Al composition between 10-95% have very low thermal conductivity compared to AlN or GaN due to the dominant phonon-alloy scattering phenomena^{25,26}. The phonon-alloy scattering decreases exponentially as the Al composition becomes >95%, thus the thermal conductivity of AlGaN enhances rapidly²⁶. Using AlGaN films (Al > 95%) with higher thermal conductivity improves heat dissipation, benefiting power electronic devices and deep UV emitters.

In both power electronics and DUV emitters, low-resistive Al-rich n-AlGaN is required to obtain ohmic contacts^{27,28}. It has been observed that obtaining ohmic contact with the Al-rich (>0.85) AlGaN is non-trivial²⁹. So, to obtain low specific contact resistivity ($<1 \mu\Omega.\text{cm}^2$), it is desired to have a significantly high n-type dopant concentration ($>10^{19}/\text{cm}^3$) such as Si in the Al-rich n-AlGaN layer. However, it has been observed that with an increase in Si doping concentration, the material quality can degrade and introduce v-pits and dislocations³⁰, which is not ideal for both power electronic and optoelectronic devices. So, developing a low-resistance Al-rich n⁺⁺-AlGaN layer with smooth surface morphology is crucial for improving the efficiency of the AlGaN-based devices.

In previous studies, regrown III-nitride materials using MOCVD have shown high unintentional Si incorporation at the regrowth interface^{31,32}. This high unintentional Si concentration ($>5 \times 10^{19}/\text{cm}^3$) can behave as deep acceptor levels causing reduced free carrier concentration in Si-doped AlN^{33,34}. So, reducing the unintentional Si incorporation or its effect would help to increase the free charge carrier concentration in regrown Si-doped thin Al-rich Al(Ga)N films.

This study demonstrated an optimized deposition condition of regrown n-type Si-doped Al-rich Al(Ga)N films on an AlN/sapphire template using a CCS MOCVD reactor to maximize free electron concentration. The effect of deposition conditions on the free electron concentration was determined. A controllable Al composition beyond 95% was observed to be difficult to achieve in the CCS reactor due to unintentional Ga incorporation. Even after increasing the Al-containing precursor flow while keeping the Ga-containing precursor flow constant, the Al composition did not increase. Thus, for obtaining 97% AlGaN, a pulsed deposition condition was pursued, rather than a continuous deposition condition. Furthermore, an unintentional Si incorporation was

observed at the interface of the AlN template and the regrown n-Al(Ga)N films, which affected the electrical performance of the n-Al(Ga)N films. A thicker Al(Ga)N layer (>300 nm) exhibited a higher free charge carrier concentration compared to a thinner layer (<100 nm). The total thickness of the Al(Ga)N layer was kept below 300 nm as obtaining a higher conductivity film with a lower thickness would be cost-effective. Finally, this work showed state-of-the-art free carrier concentration with the thinnest layer of regrown n-AlN on AlN/Sapphire template compared with the reported results from n-AlN deposited on different substrates such as bulk AlN, SiC and Sapphire.

Al-rich Al(Ga)N films (65 ± 5 nm) were deposited on AlN/sapphire templates in the CCS MOCVD reactor using triethylgallium (TEGa), trimethylaluminum (TMAI) as group-III precursors and ammonia (NH₃) as group-V precursor. Silane was used as a gaseous precursor for Si doping. First, different deposition conditions such as deposition temperatures (1050 °C, 1100 °C, 1150 °C, and 1210 °C), V/III ratio (530, 750 and 3000), deposition rate (0.52 Å/s, 0.7 Å/s, and 1 Å/s), and Si concentration (4×10^{19} /cm³, 6×10^{19} /cm³, and 8×10^{19} /cm³) were used to find the optimized deposition condition to maximize free carrier concentration of n-AlN (Table 1). The V/III ratio was varied by increasing the NH₃ flow while keeping the TMAI flow constant. To adjust the deposition rate of AlN, the TMAI flow rate was altered while maintaining a constant V/III ratio. Next, the TMAI/TEGa ratio was varied to obtain different Al compositions of Al_xGa_{1-x}N ($0.57\leq x\leq 1$) (Table 2). An Al composition over 95% was achieved with pulsed deposition, continuously supplying TMAI and NH₃, while pulsing TEGa with a 4-second ON/OFF cycle. H₂ served as the carrier gas for Al(Ga)N deposition. Finally, a thickness series of Al_{0.97}Ga_{0.03}N and AlN with thicknesses up to 280 nm was performed to understand the effect of the unintentional Si incorporation at the interface on free charge carrier concentration.

Table 1. Optimization of maximum charge carrier concentration in Si-doped AlN (65 ± 5 nm)

Experiments	Temperature (°C)	V/III ratio	Deposition Rate (Å/s)	Si (/cm ³)	n _s (/cm ³)
E _{A1}	1050	750	0.7	6×10^{19}	4×10^{13}
	1100				1×10^{14}
	1150				1.5×10^{14}
	1210				N/A
E _{A2}	1150	530	0.7	6×10^{19}	6×10^{13}
		750			1.5×10^{14}
		3000			7×10^{13}
E _{A3}	1150	750	0.52	6×10^{19}	2×10^{13}
			0.7		1.5×10^{14}
			1		1.51×10^{14}
E _{A4}	1150	750	0.7	4×10^{19}	1×10^{14}
				6×10^{19}	1.5×10^{14}
				8×10^{19}	N/A

Table 2. Variation of TMAI/TEGa ratio for obtaining different Al composition

Experiments	Temperature (°C)	V/III ratio	Deposition Rate (Å/s)	Si (/cm ³)	TMA/TEGa ratio	Al%
E _{B1}	1150	750	0.7	6×10 ¹⁹	∞	100
E _{B2}			~1		12.69	97 (Pulsed)
E _{B3}			~1		12.69	95
E _{B4}			0.92		6.43	93
E _{B5}			0.88		2.87	86
E _{B6}			1.12		0.64	57

The composition of the Al(Ga)N was measured using omega-2theta and reciprocal space mapping (RSM) techniques with the high-resolution X-ray diffraction (XRD) Panalytical Empyrean tool. The surface roughness of the Al(Ga)N films was measured by atomic force microscopy (AFM) using Bruker Icon AFM in tapping mode. The carrier concentration of the n-Al(Ga)N films was measured using mercury CV and Hall measurements using Lake Shore MCS-EMP-4T-V and the Toho HL9980 hall measurement systems. The Si concentration and Al/Ga ratio were measured by the secondary ion mass spectroscopy (SIMS) method using the Cameca SIMS measurement tool.

The Si-doped AlN films deposited at different temperatures showed a prominent trend of how the trade-off between V_{III} and C_N can be obtained in Table 1 (E_{A1}). An increase in the temperature from 1050 °C to 1150 °C, increased the free charge carrier concentration from 4×10¹³/cm³ to 1.5×10¹⁴/cm³. We speculate that this 3.75 times increase in the charge concentration may have been related to the reduction of the C_N, which acts as an acceptor-type trap. At lower deposition temperatures, C incorporation becomes very high in MOCVD-deposited III-nitride materials due to the formation of C–group-III bonds^{35–37}. The presence of the methyl groups in the TMAI was the main reason for the C incorporation. Increasing the temperature promotes the elimination of C from the group-III element by breaking the C–group-III bonds. A sharp decrease in the carrier concentration was observed when the deposition temperature was increased beyond 1150 °C. It was demonstrated previously in the literature that with increasing deposition temperature, the V_{III} formation increases^{22,36,37}. So, the probability of V_{III}-Si complex formation increases rapidly. Thus, the sharp decrease in carrier concentration was presumably related to the V_{III}-Si complex formation, like the trend observed by *Washiyama et al.*^{36,37}. As the maximum charge was observed at 1150 °C, the rest of the experiments were performed at 1150 °C.

In the next set of experiments, the V/III ratio was varied from 530 to 3000 to identify the effect of C_N and N vacancy formation on the free charge carrier concentration, as shown in Table 1 (E_{A2}). At a low V/III ratio (530), the N vacancy formation probably increased which enhanced the C incorporation in the N sites, forming C_N³⁶. It caused a lower charge carrier concentration of 6×10¹³/cm³. When the V/III ratio was increased from 530 to 750, the charge increased by 2.5

times, reaching $1.5 \times 10^{14}/\text{cm}^3$, indicating less C_N formation. However, a high V/III ratio (3000) decreased the charge carrier concentration again from $1.5 \times 10^{14}/\text{cm}^3$ to $7 \times 10^{13}/\text{cm}^3$. We speculate that the reduction in the charge carrier concentration was related to the increased group-III vacancy formation with increased NH_3 ³⁶.

Next, the effect of the deposition rate on the charge carrier concentration was observed, shown in Table 1 (E_{A3}). The increase in deposition rate from 0.57 Å/s to 0.72 Å/s showed an increase in the charge concentration from $2 \times 10^{13}/\text{cm}^3$ to $1.5 \times 10^{14}/\text{cm}^3$. We speculate that an increment in deposition rate helped to reduce the desorption of group-III species, thus the V_{III} formation got suppressed, and a similar phenomenon has been observed for high-composition n-AlGaIn layers as reported by another group in ref. ³⁸. However, with increasing TMAI flow rate the unintentional C concentration also increases, thus the chances of C_N formation also increase^{35,38,39}. So, a very high TMAI flow rate would cause detrimental effects in terms of film conductivity. A further increase in the deposition rate from 0.72 Å/s to 1 Å/s, did not increase the charge carrier concentration significantly, which might be due to the trade-off between reduced V_{III} and increased C_N concentration with increasing TMAI flow rate³⁸. Further increments in the TMAI flow rate can increase C_N formation. Thus, the deposition rate was maintained at 0.7 Å/s to avoid excess C_N formation.

Next, a silicon concentration variation was performed to identify the optimal Si concentration needed to obtain the highest charge in the AlN layers as shown in Table 1 (E_{A4}). As expected, increasing the Si concentration from $4 \times 10^{19}/\text{cm}^3$ to $6 \times 10^{19}/\text{cm}^3$ increased the charge concentration from $10^{14}/\text{cm}^3$ to $1.5 \times 10^{14}/\text{cm}^3$. However, increasing Si concentration from $6 \times 10^{19}/\text{cm}^3$ to $8 \times 10^{19}/\text{cm}^3$ decreased the charge concentration sharply, indicating the self-compensation phenomena of Si^{36,37}. At very high Si concentrations, the V_{III} -Si complex formation, which acts as a compensator, becomes more energetically favorable³⁶. Thus, the concentration of the V_{III} -Si complex increases at very high Si concentration, causing enhanced compensation of free charge carriers leading to the self-compensation phenomenon of Si³⁶. So, a Si concentration of $6 \times 10^{19}/\text{cm}^3$ was chosen to be optimal.

After optimizing the deposition condition for the Si-doped AlN, different Al composition AlGaIn films were deposited to identify the charge incorporation efficiency in different alloy compositions. It was observed that the charge incorporation efficiency exponentially increased with the increase of Ga mole fraction in AlGaIn⁴⁰. Nearly 5 orders of magnitude increase in charge carrier concentration was observed when the Ga mole fraction increased from 0 to 43% (Figure 1). Also, the mobility of the Al(Ga)In film increased from $\sim 7 \text{ cm}^2/\text{Vs}$ to $45 \text{ cm}^2/\text{Vs}$ with increasing Ga mole fraction from 0% to 43%. Obtaining AlGaIn with <5% Ga was not trivial in the CCS reactor, as it was observed that the Ga mole fraction saturated at 5%. With increasing TMAI flow by 38%, the Ga mole fraction could not be lowered further while both the TMAI and TEGa precursors were continuously flowing into the deposition chamber (continuous deposition mode). This saturation of Ga incorporation was mostly related to the unintentional Ga incorporation in the reactor chamber, as also reported elsewhere^{23,24}. So, for obtaining Al_{0.97}Ga_{0.03}In, the pulsed deposition condition was used as described in the experimental methods section.

AFM scans showed that with a reduction of Ga composition, surface roughness increased for Al(Ga)N films (65 ± 5 nm) deposited with continuous deposition mode. However, a clear difference in the surface roughness was observed between the continuous deposition mode and the pulsed deposition mode thin films. The pulsed deposition mode showed almost 4 times lower surface roughness (0.42 nm) compared to all the continuous mode samples (trend line) (Figure 2). We speculate the pulsed mode deposition increased the diffusion length of the group-III adatoms which helped to improve the surface roughness⁴¹.

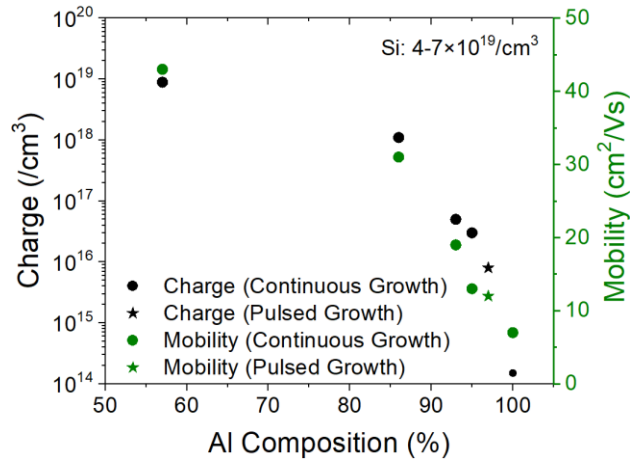


Figure 1. Charge concentration in different Al compositions of Al(Ga)N films (65 ± 5 nm) with a Si concentration between $4-7\times 10^{19}/\text{cm}^3$

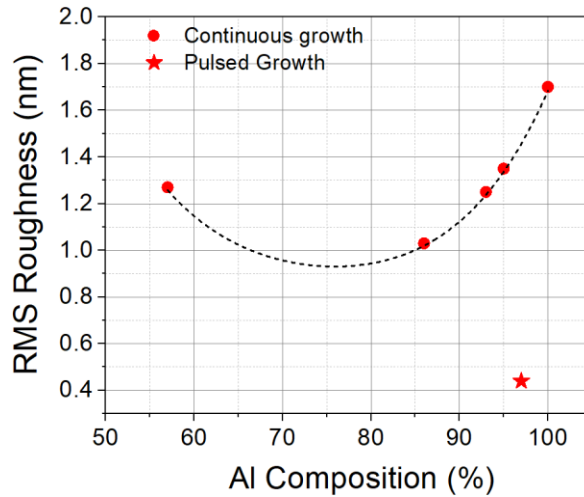


Figure 2. Effect of the surface roughness (AFM scan of $10\times 10\ \mu\text{m}^2$) of the Al(Ga)N films (65 ± 5 nm) with different compositions of the Al and different deposition modes

The SIMS measurement of Si-doped AlN showed very high unintentional Si incorporation at the interface between the regrown AlN and the AlN template (Figure 3a). This closely resembled the high unintentional silicon incorporation observed in regrown GaN films using MOCVD, as documented in the literature^{31,32}. The unintentional Si incorporation was related to the presence

of the residual Si in the MOCVD chamber as reported previously³². It was hypothesized that this high unintentional silicon incorporation led to carrier compensation^{33,34}, and therefore in our case, as the thickness of the Al(Ga)N layer increased, the concentration of free charge carriers also increased with lower carrier compensation away from the regrowth interface. This indicated that the Si-doping which was used in our regrown Al(Ga)N layers was optimal and the actual doping efficiency was higher than the measured values for the samples with a lower regrown layer thickness (65 ± 5 nm). The charge concentration increased by ~ 6 times for $\text{Al}_{0.97}\text{Ga}_{0.03}\text{N}$, with 4 times increase in thickness reaching $4.8\times 10^{16}/\text{cm}^3$, reaching the highest reported free carrier concentration in 97% n-AlGa_{0.03}N. Similarly, for AlN, the charge was enhanced by almost 50 times achieving $7.5\times 10^{15}/\text{cm}^3$ while the thickness was increased by 3 times (Figure 3b). This demonstrates that the compensation effect of the unintentional Si incorporation was more drastic in AlN compared to $\text{Al}_{0.97}\text{Ga}_{0.03}\text{N}$. We think that this phenomenon was related to the higher probability of forming the DX^{-1} state of the Si and $\text{V}_{\text{III}}\text{-Si}$ complex in n-AlN, which severely affects the free electron concentration in n-AlN films compared to n-AlGa_{0.03}N⁴².

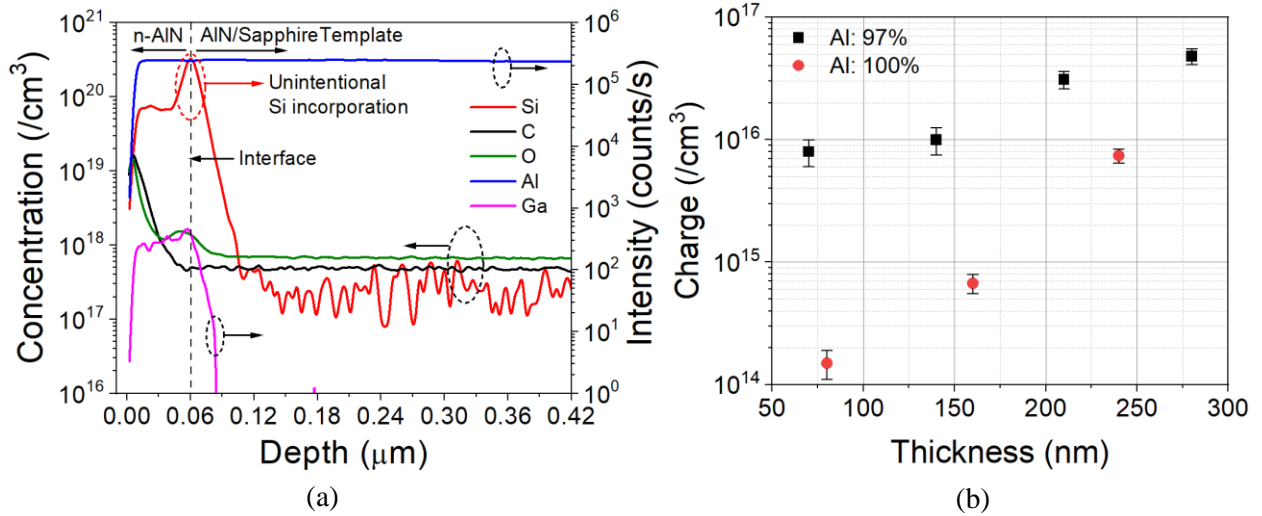


Figure 3. (a) SIMS measurement of Si-doped AlN (65 ± 5 nm) film (b) Thickness vs charge concentration for $\text{Al}_{0.97}\text{Ga}_{0.03}\text{N}$ and AlN films

The SIMS measurement of the Al(Ga)N films (65 ± 5 nm) showed that for AlN the Al/Ga ratio was ~ 1000 . This proves that the unintentional Ga incorporation in AlN was ($\sim 0.1\%$), which was below the alloy level⁴³. Finally, the AFM measurement of 280 nm n- $\text{Al}_{0.97}\text{Ga}_{0.03}\text{N}$ and 240 nm n-AlN showed smooth surface morphology with a surface roughness of 0.56 nm and 0.13 nm ($2\ \mu\text{m}\times 2\ \mu\text{m}$), respectively (Figure 4). A larger v-pit depth of ~ 25 nm was observed in n- $\text{Al}_{0.97}\text{Ga}_{0.03}\text{N}$ compared to ~ 1 nm in n-AlN, which was the reason behind the increased roughness in $\text{Al}_{0.97}\text{Ga}_{0.03}\text{N}$. The large difference in v-pit depth between n- $\text{Al}_{0.97}\text{Ga}_{0.03}\text{N}$ and n-AlN films with similar Si doping concentrations ($6\times 10^{19}/\text{cm}^3$) is still under investigation and might be related to the difference in film thickness.

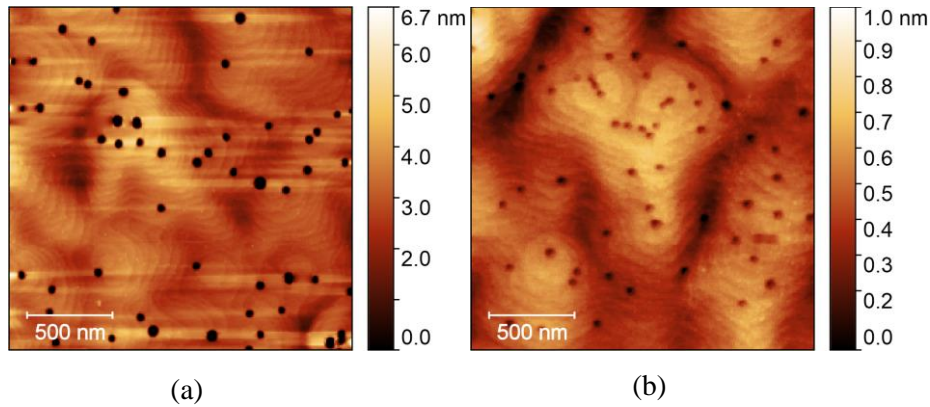


Figure 4. AFM image ($2\ \mu\text{m}\times 2\ \mu\text{m}$) of (a) 280 nm $n\text{-Al}_{0.97}\text{Ga}_{0.03}\text{N}$ ($R_a=0.56\ \text{nm}$) and (b) 240 nm $n\text{-AlN}$ ($R_a=0.13\ \text{nm}$)

The obtained free charge carrier concentration in Si-doped AlN measured using Hall measurement was compared with the state-of-the-art $n\text{-AlN}$ films deposited using MOCVD as reported in the literature (Figure 5). A high free carrier concentration of $7.5\times 10^{15}\ \text{/cm}^3$ with the lowest AlN thickness (240 nm) was demonstrated in this study (Figure 5). This is especially useful for regrown n^{++} AlN contact development for AlN or Al-rich AlGa N -based power devices. Also, it provides insight into further development of the interface quality at the regrown AlN layer and the AlN on sapphire template junction, to help further increase the free carrier concentration. However, the mobility was still below $10\ \text{cm}^2/\text{V}\cdot\text{s}$, which needs to be improved significantly by reducing the dislocation density, as reported previously^{37,44}.

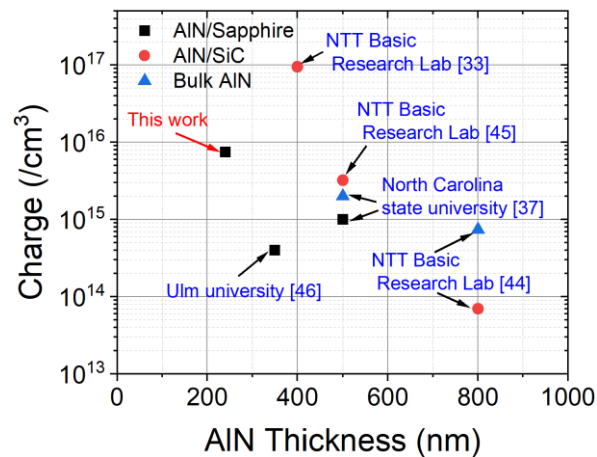


Figure 5. Comparative study of the free charge carrier concentration with AlN thickness for different AlN templates

In conclusion, this study demonstrates methods to obtain high free carrier concentrations in Si-doped high composition ($\text{Al}>90\%$) AlGa N using a commercially available CCS reactor by optimizing deposition temperature, V/III ratio, deposition rate, and Si concentration. The pulsed deposition method was used to obtain 97% AlGa N in a CCS reactor with a very low surface

roughness of 0.42 nm (scan area of $10 \times 10 \mu\text{m}^2$) and a charge concentration of $4.8 \times 10^{16} / \text{cm}^3$, which is the highest carrier concentration reported so far. Moreover, the effect of the unintentional Si incorporation at the regrown AlN and AlN on sapphire template interface was explored, and it was found that increasing the thickness of the regrown AlN thickness helps to increase free carrier concentrations. A maximum free carrier concentration of $7.5 \times 10^{15} / \text{cm}^3$ was obtained with 240 nm regrown AlN on the AlN on sapphire templates. Further reduction of DX state formation, Si self-compensation and $V_{\text{III-Si}}$ complex formation would greatly improve the charge concentration in n-AlN films in the future, which would be crucial for AlN-based power devices and deep UV emitters.

Acknowledgment:

The authors gratefully acknowledge Lake Shore Cryotronics and Toho Technology for providing the Hall measurement results. The research is partially funded by the NSF CAREER (ECCS-2338683), NSF ASCENT (ECCS-2328137) and ARPA-E ULTRAFast (AWD00001917).

References:

- ¹ S. Bajaj, A. Allerman, A. Armstrong, T. Razzak, V. Talesara, W. Sun, S.H. Sohel, Y. Zhang, W. Lu, A.R. Arehart, F. Akyol, and S. Rajan, "High Al-Content AlGa_N Transistor With 0.5 A/mm Current Density and Lateral Breakdown Field Exceeding 3.6 MV/cm," *IEEE Electron Device Lett.* **39**(2), 256–259 (2018).
- ² I. Abid, R. Kabouche, F. Medjdoub, S. Besendorfer, E. Meissner, J. Derluyn, S. Degroote, M. Germain, and H. Miyake, "Remarkable Breakdown Voltage on AlN/AlGa_N/AlN double heterostructure," in *2020 32nd International Symposium on Power Semiconductor Devices and ICs (ISPSD)*, (IEEE, Vienna, Austria, 2020), pp. 310–312.
- ³ J. Mehta, I. Abid, R. Elwaradi, Y. Cordier, and F. Medjdoub, "Robust Al_{0.23}Ga_{0.77}N channel HFETs on bulk AlN for high voltage power electronics," *E-Prime - Advances in Electrical Engineering, Electronics and Energy* **5**, 100263 (2023).
- ⁴ D.H. Mudiyansele, D. Wang, B. Da, Z. He, and H. Fu, "Over 600 V Lateral AlN-on-AlN Schottky Barrier Diodes with Ultra-Low Ideality Factor," *Appl. Phys. Express* **17**(7), 074001 (2024).
- ⁵ D.H. Mudiyansele, D. Wang, B. Da, Z. He, and H. Fu, "High-voltage AlN Schottky barrier diodes on bulk AlN substrates by MOCVD," *Appl. Phys. Express* **17**(1), 014005 (2024).
- ⁶ K. Hussain, A. Mamun, R. Floyd, M.D. Alam, M.E. Liao, K. Huynh, Y. Wang, M. Goorsky, M.V.S. Chandrashekhara, G. Simin, and A. Khan, "High figure of merit extreme bandgap Al_{0.87}Ga_{0.13}N-Al_{0.64}Ga_{0.36}N heterostructures over bulk AlN substrates," *Appl. Phys. Express* **16**(1), 014005 (2023).
- ⁷ B.K. SaifAddin, A.S. Almogbel, C.J. Zollner, F. Wu, B. Bonef, M. Iza, S. Nakamura, S.P. DenBaars, and J.S. Speck, "AlGa_N Deep-Ultraviolet Light-Emitting Diodes Grown on SiC Substrates," *ACS Photonics* **7**(3), 554–561 (2020).
- ⁸ N. Lobo-Ploch, F. Mehnke, L. Sulmoni, H.K. Cho, M. Guttmann, J. Glaab, K. Hilbrich, T. Wernicke, S. Einfeldt, and M. Kneissl, "Milliwatt power 233 nm AlGa_N-based deep UV-LEDs on sapphire substrates," *Appl. Phys. Lett.* **117**(11), (2020).
- ⁹ Z. Zhang, M. Kushimoto, A. Yoshikawa, K. Aoto, C. Sasaoka, L.J. Schowalter, and H. Amano, "Key temperature-dependent characteristics of AlGa_N-based UV-C laser diode and demonstration of room-temperature continuous-wave lasing," *Appl. Phys. Lett.* **121**(22), (2022).
- ¹⁰ Z. Zhang, M. Kushimoto, M. Horita, N. Sugiyama, L.J. Schowalter, C. Sasaoka, and H. Amano, "Space charge profile study of AlGa_N-based p-type distributed polarization doped claddings without impurity doping for UV-C laser diodes," *Appl. Phys. Lett.* **117**(15), (2020).

- ¹¹ I. Bryan, Z. Bryan, S. Washiyama, P. Reddy, B. Gaddy, B. Sarkar, M.H. Breckenridge, Q. Guo, M. Bobeia, J. Tweedie, S. Mita, D. Irving, R. Collazo, and Z. Sitar, “Doping and compensation in Al-rich AlGa_xN grown on single crystal AlN and sapphire by MOCVD,” *Appl. Phys. Lett.* **112**(6), (2018).
- ¹² H. Ahmad, Z. Engel, C.M. Matthews, S. Lee, and W.A. Doolittle, “Realization of homojunction PN AlN diodes,” *J. Appl. Phys.* **131**(17), (2022).
- ¹³ P. Bagheri, A. Klump, S. Washiyama, M. Hayden Breckenridge, J.H. Kim, Y. Guan, D. Khachariya, C. Quiñones-García, B. Sarkar, S. Rathkanthiwar, P. Reddy, S. Mita, R. Kirste, R. Collazo, and Z. Sitar, “Doping and compensation in heavily Mg doped Al-rich AlGa_xN films,” *Appl. Phys. Lett.* **120**(8), (2022).
- ¹⁴ H. Ahmad, J. Lindemuth, Z. Engel, C.M. Matthews, T.M. McCrone, and W.A. Doolittle, “Substantial P-Type Conductivity of AlN Achieved via Beryllium Doping,” *Advanced Materials* **33**(42), 2104497 (2021).
- ¹⁵ M.E. Zvanut, J.P. Hanle, S. Paudel, R. Page, C. Savant, Y. Cho, H.G. Xing, and D. Jena, “An electron paramagnetic resonance study of the electron transport in heavily Si-doped high Al content Al_xGa_{1-x}N,” *AIP Advances* **13**(12), (2023).
- ¹⁶ I. Prozheev, F. Mehnke, T. Wernicke, M. Kneissl, and F. Tuomisto, “Electrical compensation and cation vacancies in Al rich Si-doped AlGa_xN,” *Appl. Phys. Lett.* **117**(14), (2020).
- ¹⁷ M.S. Brandt, R. Zeisel, S.T.B. Gönnerwein, M.W. Bayerl, and M. Stutzmann, “DX behaviour of Si donors in AlGa_xN alloys,” *Physica Status Solidi (b)* **235**(1), 13–19 (2003).
- ¹⁸ X.T. Trinh, D. Nilsson, I.G. Ivanov, E. Janzén, A. Kakanakova-Georgieva, and N.T. Son, “Stable and metastable Si negative-U centers in AlGa_xN and AlN,” *Appl. Phys. Lett.* **105**(16), (2014).
- ¹⁹ J. Wang, F. Xu, L. Zhang, J. Lang, X. Fang, Z. Zhang, X. Guo, C. Ji, C. Ji, F. Tan, X. Yang, X. Kang, Z. Qin, N. Tang, X. Wang, W. Ge, and B. Shen, “Progress inefficient doping of Al-rich AlGa_xN,” *J. Semicond.* **45**(2), 021501 (2024).
- ²⁰ M.I. Khan, C. Lee, and E. Ahmadi, “Demonstration of controllable Si doping in N-polar AlN using plasma-assisted molecular beam epitaxy,” *Appl. Phys. Lett.* **124**(6), (2024).
- ²¹ J. Stellmach, M. Pristovsek, Ö. Savaş, J. Schlegel, E.V. Yakovlev, and M. Kneissl, “High aluminium content and high growth rates of AlGa_xN in a close-coupled showerhead MOVPE reactor,” *Journal of Crystal Growth* **315**(1), 229–232 (2011).
- ²² I. Prozheev, F. Mehnke, T. Wernicke, M. Kneissl, and F. Tuomisto, “Electrical compensation and cation vacancies in Al rich Si-doped AlGa_xN,” *Appl. Phys. Lett.* **117**(14), (2020).
- ²³ G. Deng, L. Zhang, Y. Wang, J. Yu, Y. Niu, H. Qian, X. Li, Z. Shi, and Y. Zhang, “Ga-free AlInN films growth by close-coupled showerhead metalorganic chemical vapor deposition,” *Micro and Nanostructures* **165**, 207191 (2022).
- ²⁴ M. Mrad, Y. Mazel, G. Feuillet, and M. Charles, “Avoiding Gallium Pollution in Close-Coupled Showerhead Reactors, Alternative Process Routes,” *Physica Status Solidi (a)* **220**(16), 2200824 (2023).
- ²⁵ W. Liu, and A.A. Balandin, “Thermal conduction in Al_xGa_{1-x}N alloys and thin films,” *J. Appl. Phys.* **97**(7), (2005).
- ²⁶ D.Q. Tran, R.D. Carrascon, M. Iwaya, B. Monemar, V. Darakchieva, and P.P. Paskov, “Thermal conductivity of Al_xGa_{1-x}N (0≤x≤1) epitaxial layers,” *Phys. Rev. Mater.* **6**(10), 104602 (2022).
- ²⁷ M. Hiroki, Y. Taniyasu, and K. Kumakura, “High-Temperature Performance of AlN MESFETs With Epitaxially Grown n-Type AlN Channel Layers,” *IEEE Electron Device Lett.* **43**(3), 350–53, (2022).
- ²⁸ M. Kneissl, T.-Y. Seong, J. Han, and H. Amano, “The emergence and prospects of deep-ultraviolet light-emitting diode technologies,” *Nat. Photonics* **13**(4), 233–244 (2019).
- ²⁹ R. France, T. Xu, P. Chen, R. Chandrasekaran, and T.D. Moustakas, “Vanadium-based Ohmic contacts to n-AlGa_xN in the entire alloy composition,” *Appl. Phys. Lett.* **90**(6), (2007).
- ³⁰ D. Nilsson, E. Janzén, and A. Kakanakova-Georgieva, “Strain and morphology compliance during the intentional doping of high-Al-content AlGa_xN layers,” *Appl. Phys. Lett.* **105**(8), (2014).
- ³¹ K. Fu, H. Fu, X. Deng, P.-Y. Su, H. Liu, K. Hatch, C.-Y. Cheng, D. Messina, R.V. Meidanshahi, P. Peri, C. Yang, T.-H. Yang, J. Montes, J. Zhou, X. Qi, S.M. Goodnick, F.A. Ponce, D.J. Smith, R. Nemanich, and Y. Zhao, “The impact of interfacial Si contamination on GaN-on-GaN regrowth for high power vertical devices,” *Appl. Phys. Lett.* **118**(22), (2021).

- ³² M. Noshin, R. Soman, X. Xu, and S. Chowdhury, “A systematic study of the regrown interface impurities in unintentionally doped Ga-polar c-plane GaN and methods to reduce the same,” *Semicond. Sci. Technol.* **37**(7), 075018 (2022).
- ³³ Y. Taniyasu, M. Kasu, and N. Kobayashi, “Intentional control of n-type conduction for Si-doped AlN and Al_xGa_{1-x}N (0.42 ≤ x < 1),” *Appl. Phys. Lett.* **81**(7), 1255–1257 (2002).
- ³⁴ F. Mehnke, X.T. Trinh, H. Pingel, T. Wernicke, E. Janzén, N.T. Son, and M. Kneissl, “Electronic properties of Si-doped Al_xGa_{1-x}N with aluminum mole fractions above 80%,” *J. Appl. Phys.* **120**(14), (2016).
- ³⁵ A.S. Almogbel, C.J. Zollner, B.K. Saifaddin, M. Iza, J. Wang, Y. Yao, M. Wang, H. Foronda, I. Prozhnev, F. Tuomisto, A. Albadri, S. Nakamura, S.P. DenBaars, and J.S. Speck, “Growth of highly conductive Al-rich AlGa_N:Si with low group-III vacancy concentration,” *AIP Advances* **11**(9), (2021).
- ³⁶ S. Washiyama, P. Reddy, B. Sarkar, M.H. Breckenridge, Q. Guo, P. Bagheri, A. Klump, R. Kirste, J. Tweedie, S. Mita, Z. Sitar, and R. Collazo, “The role of chemical potential in compensation control in Si:AlGa_N,” *J. Appl. Phys.* **127**(10), (2020).
- ³⁷ P. Bagheri, C. Quiñones-García, D. Khachariya, S. Rathkanthiwar, P. Reddy, R. Kirste, S. Mita, J. Tweedie, R. Collazo, and Z. Sitar, “High electron mobility in AlN:Si by point and extended defect management,” *J. Appl. Phys.* **132**(18), (2022).
- ³⁸ J. Yang, Y.H. Zhang, D.G. Zhao, P. Chen, Z.S. Liu, and F. Liang, “Realization low resistivity of high AlN mole fraction Si-doped AlGa_N by suppressing the formation native vacancies,” *Journal of Crystal Growth* **570**, 126245 (2021).
- ³⁹ D.D. Koleske, A.E. Wickenden, R.L. Henry, and M.E. Twigg, “Influence of MOVPE growth conditions on carbon and silicon concentrations in GaN,” *Journal of Crystal Growth* **242**(1–2), 55–69 (2002).
- ⁴⁰ F. Mehnke, T. Wernicke, H. Pingel, C. Kuhn, C. Reich, V. Kueller, A. Knauer, M. Lapeyrade, M. Weyers, and M. Kneissl, “Highly conductive n-Al_xGa_{1-x}N layers with aluminum mole fractions above 80%,” *Appl. Phys. Lett.* **103**(21), (2013).
- ⁴¹ I. Ahmad, B. Krishnan, B. Zhang, Q. Fareed, M. Lachab, J. Dion, and A. Khan, “Dislocation reduction in high Al-content AlGa_N films for deep ultraviolet light emitting diodes,” *Physica Status Solidi (a)* **208**(7), 1501–1503 (2011).
- ⁴² T.A. Henry, A. Armstrong, A.A. Allerman, and M.H. Crawford, “The influence of Al composition on point defect incorporation in AlGa_N,” *Appl. Phys. Lett.* **100**(4), (2012).
- ⁴³ M.I. Khan, C. Lee, and E. Ahmadi, “Demonstration of controllable Si doping in N-polar AlN using plasma-assisted molecular beam epitaxy,” *Appl. Phys. Lett.* **124**(6), (2024).
- ⁴⁴ Y. Taniyasu, M. Kasu, and T. Makimoto, “Increased electron mobility in n-type Si-doped AlN by reducing dislocation density,” *Appl. Phys. Lett.* **89**(18), (2006).
- ⁴⁵ Y. Taniyasu, M. Kasu, and T. Makimoto, “Electrical conduction properties of n-type Si-doped AlN with high electron mobility (>100cm²V⁻¹s⁻¹),” *Appl. Phys. Lett.* **85**(20), 4672–4674 (2004).
- ⁴⁶ S.B. Thapa, J. Hertkorn, F. Scholz, G.M. Prinz, R.A.R. Leute, M. Feneberg, K. Thonke, R. Sauer, O. Klein, J. Biskupek, and U. Kaiser, “Growth and studies of Si-doped AlN layers,” *Journal of Crystal Growth* **310**(23), 4939–4941 (2008).